

PAPER • OPEN ACCESS

## Magnetic Flux Trapping and Flux Jumps in Pulsed Field Magnetizing Processes in REBCO and Mg-B Bulk Magnets

To cite this article: T Oka *et al* 2020 *J. Phys.: Conf. Ser.* **1590** 012025

View the [article online](#) for updates and enhancements.

A promotional banner for the 240th ECS Meeting. The banner features a colorful striped border at the top. On the left, the ECS logo is displayed in a green circle. To its right, the text reads "240th ECS Meeting" in large blue font, followed by "Oct 10-14, 2021, Orlando, Florida" in a smaller blue font. Below this, it says "Register early and save up to 20% on registration costs" in bold black font, and "Early registration deadline Sep 13" in a smaller black font. At the bottom left, there is a red "REGISTER NOW" button. On the right side of the banner, there is a photograph of a diverse group of people in professional attire, smiling and clapping, suggesting a successful event or presentation.

**ECS** **240th ECS Meeting**  
Oct 10-14, 2021, Orlando, Florida  
**Register early and save  
up to 20% on registration costs**  
Early registration deadline Sep 13  
**REGISTER NOW**

# Magnetic Flux Trapping and Flux Jumps in Pulsed Field Magnetizing Processes in REBCO and Mg-B Bulk Magnets

T Oka<sup>1</sup>, A Takeda<sup>2</sup>, H Oki<sup>2</sup>, K Yamanaka<sup>1</sup>, L Dadiel<sup>1</sup>, K Yokoyama<sup>3</sup>,  
W Häbler<sup>4</sup>, J Scheiter<sup>4</sup>, N Sakai<sup>1</sup> and M Murakami<sup>1</sup>

<sup>1</sup> Shibaura Institute of Technology, 3-7-5 Toyosu, Koto-Ward, Tokyo 135-8548, Japan

<sup>2</sup> Niigata University, 8050 Ikarashi-Ninocho, Nishi-Ward, Niigata 950-8151, Japan,

<sup>3</sup> Ashikaga University, 268-1 Omae-cho, Ashikaga 326-8558, Japan

<sup>4</sup> IFW Dresden, 20 Helmholtzstr., Dresden 01069, Germany

E-mail: okat@sic.shibaura-it.ac.jp

**Abstract.** Pulsed-field magnetization technique (PFM) is expected as a cheap and an easy way for HTS bulk materials for utilizing as intense magnets. As the generation of heat due to magnetic flux motion in bulk magnets causes serious degradation of captured fields, it is important to investigate the flux motions during PFM in various field applications. The authors precisely measured the magnetic flux motion in the cryocooled MgB<sub>2</sub> bulk magnets containing various amount of Ti. We classified the motions to “no flux flow (NFF)”, “fast flux flow (FFF)”, and “flux jump (FJ)” regions. The results showed that addition of Ti shifts the field invasion area to high field areas, and expands the NFF regions. The highest field-trapping appears at the upper end of the NFF region. Since the heat generation and its propagation should attribute to the dissipation of magnetic flux, FFF leads to FJ. Compared with MgB<sub>2</sub>, we referred to GdBCO as for the flux motion. A flux jump was observed at 30 K when the pulse field of 7 T was applied to the preactivated sample, showing its stability against FJ.

## 1. Introduction

The largely-grown high temperature superconducting bulk materials (hereafter abbreviated as HTS bulk magnet or bulk magnet) are capable of acting as quasi permanent magnets under their superconducting state. We call them as HTS bulk magnets or the trapped field magnets (TFM) [1], [2]. Since the principle of field trapping is different from that of conventional permanent magnets like Nd-Fe-B or ferrite magnets, we can obtain extraordinary intense magnets when they are activated by superconducting solenoid magnets [3], [4] or the pulsed-field magnetizing (PFM) technique [5], [6]. The captured field is very stable when it is cooled far beneath the critical temperature [7]. Since the field-trapping ability linearly increases with lowering temperature, it is important to cool the bulk magnets under 77 K by adopting cryocoolers [8] [9]. Then, the enhancement of mechanical toughness is necessary to endure the strong hoop stress caused by capturing the magnetic flux inside the materials [10].

The practical application candidates for TFM such as NMR magnets or other small-sized field generators require the extremely-uniform magnetic field distribution [11], [12]. MgB<sub>2</sub> is surely one of the promising candidates capable of generating uniform magnetic field distribution due to its homogeneous microstructure in spite of lower  $T_c$  than RE-Ba-Cu-O (or REBCO, RE: rare earth elements) compounds [13]. As far as we adopt the TFMs made of MgB<sub>2</sub>, we need to prepare two-stage



**Table 1.** MgB<sub>2</sub> sample preparation.

Sample	Diameter d (mm)	Thickness t (mm)	Aspect ratio d/t	Density g/cm <sup>3</sup>	Mg : B (Molar ratio)
Ti-0% (MH90-2,3,7,4,5)	20	6.08	3.29	-	1 : 2 (Pristine)
Ti-2.5% (MH104b,c)	20	6.45	3.1	2.31 2.41	1 : 2 (2.5wt%Ti)
Ti-5.0% (MH113a,b)	20	6.57	3.0	2.50	1 : 2 (5.0wt%Ti)

GM-cycle cryocoolers and magnetizing tools such as superconducting solenoid magnets or pulsed field coils [14].

As pointed in the past papers, the thermal property such as low specific heat and high thermal propagation coefficient originated from “metallic” MgB<sub>2</sub> compound might cause serious flux-jump phenomena in PFM processes. Due to the narrow temperature margin between the operating temperature and  $T_c = 39$  K [15], [16], the PFM process has a problem which would degrade the  $J_c$  value by heat generation caused by the flux motion. The lower  $T_c$  than that of REBCO pushes the operation temperature down, which leads to the low heat capacity and crucial temperature rises. In the study, the authors analyze various flux jump behavior and clarify its mechanism. We aim to improve the thermal stability to prevent the flux jumps by examining Ti addition, and estimate the realms of flux jump kingdom.

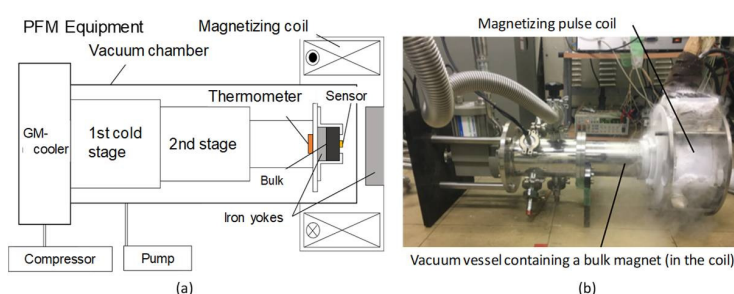
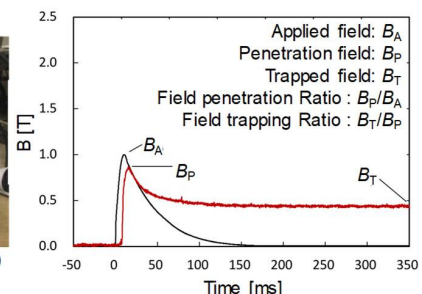
## 2. Experimental procedure

### 2.1. Preparation of MgB<sub>2</sub> bulk samples

The samples with various Ti contents were prepared by the hot-pressing process in IFW Dresden in attendance with the students from Japan. As it was clarified that the total sample thickness influences on the shielding effect against the invading flux [16], [17], the thin plates were unified to around 6.5 mm in thickness by stacking them. Table 1 shows their specifications, including the illustrations of sample setups on the cold stage. The detailed conditions were shown elsewhere [16], [17]. The Ti contents were chosen as 0wt% (pristine), 2.5wt%, and 5.0wt%. After ball-milling for 10h, the precursors were sintered by hot-pressing with applying pressure of 480 and 640 MPa for pristine and Ti-doped samples, respectively. Then, they were heat-treated at 700 °C for 10 min.

### 2.2 Pulsed field magnetization and magnetic flux motions

Figure 1 shows the illustration and photo of the experimental setup for the PFM, employing the two-stage GM cooler. The bulk samples were cooled to operating temperature of 14.6-14.8 K for the pristine and 13 K for Ti-doped samples, respectively. The magnetic field data were measured at the center of the bulk surface by a Hall sensor.

**Figure 1.** Experimental setup.**Figure 2.** Definition of parameters.

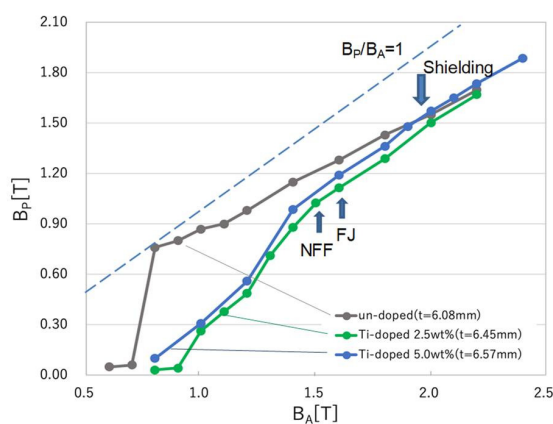


**Figure 3.** Penetration field  $B_p$ .

condenser to the cryocooled bulk  $\text{MgB}_2$  samples with use of 112-turn copper coil. The coil is cooled in the liquid nitrogen vessel to reduce its resistance. The coil constant is 1.26 mT/A.

### 2.3 GdBCO sample and its magnetic flux motion

A melt-processed GdBCO sample was prepared to compare the flux-jump phenomena. The size of which was 30 mm in diameter and 10 mm in thickness. The  $T_c$  value is 90 K. The single stage GM cooler cooled the sample to 30 K. The successive magnetic fields around 5-7 T were applied to the bulk magnets as a same manner as Mg-B bulk sample [19]. The time dependence of the magnetic flux density was measured at the surface center by a Hall sensor during PFM operations.

## 3. Results and Discussion

### 3.1 Penetration fields

Figure 3 shows the applied field dependence of the penetration fields  $B_p$  as a function of Ti contents. All the lines deviated beneath the line of  $B_p/B_A=1$ , which suggest strong shielding effects on this stacked thick samples. The data points of the pristine sample were a bit different from others in the range less than 1.4 T. This may imply the effect of Ti-addition to the shielding against the flux invasion.

### 3.2 Trapped field and field trapping ratio

Figure 4 and 5 show the data of trapped field  $B_T$  and the field trapping ratio  $B_T/B_p$  for the samples with various Ti contents. We see the magnetic flux started invading at 0.7 T for the pristine and at 1.0 T for

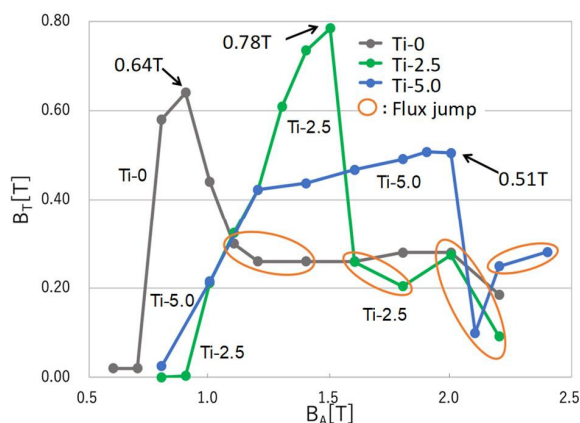


**Figure 4.** Trapped field  $B_T$ .

The authors introduced the definitions of parameters of field penetration ratio  $B_p/B_A$  and field trapping ratio  $B_T/B_p$ , as indicated in Figure 2, to prepare for the following discussion (ref. [18]). The values of  $B_A$  and  $B_p$  correspond to the highest peaks of applied fields and flux penetrations, respectively.  $B_T$  means the final trapped field at the end of PFM profiles.

The ratio of  $B_p/B_A$  indicates the shielding effect which estimates the flux motion to invade into the sample. The ratio of  $B_T/B_p$ , indicating the flux-trapping ability, strongly reflects the heat generation and its propagation in the sample. The pulse-fields of 0.6 - 2.4 T with a rise time of 10 ms were applied by feeding current from 60 mF

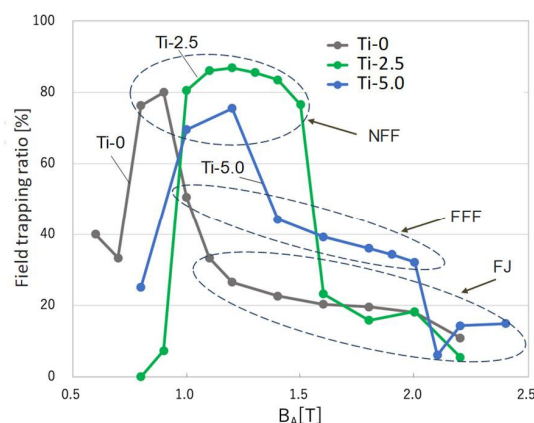


**Figure 5.** Field-trapping ratio  $B_T/B_p$ .

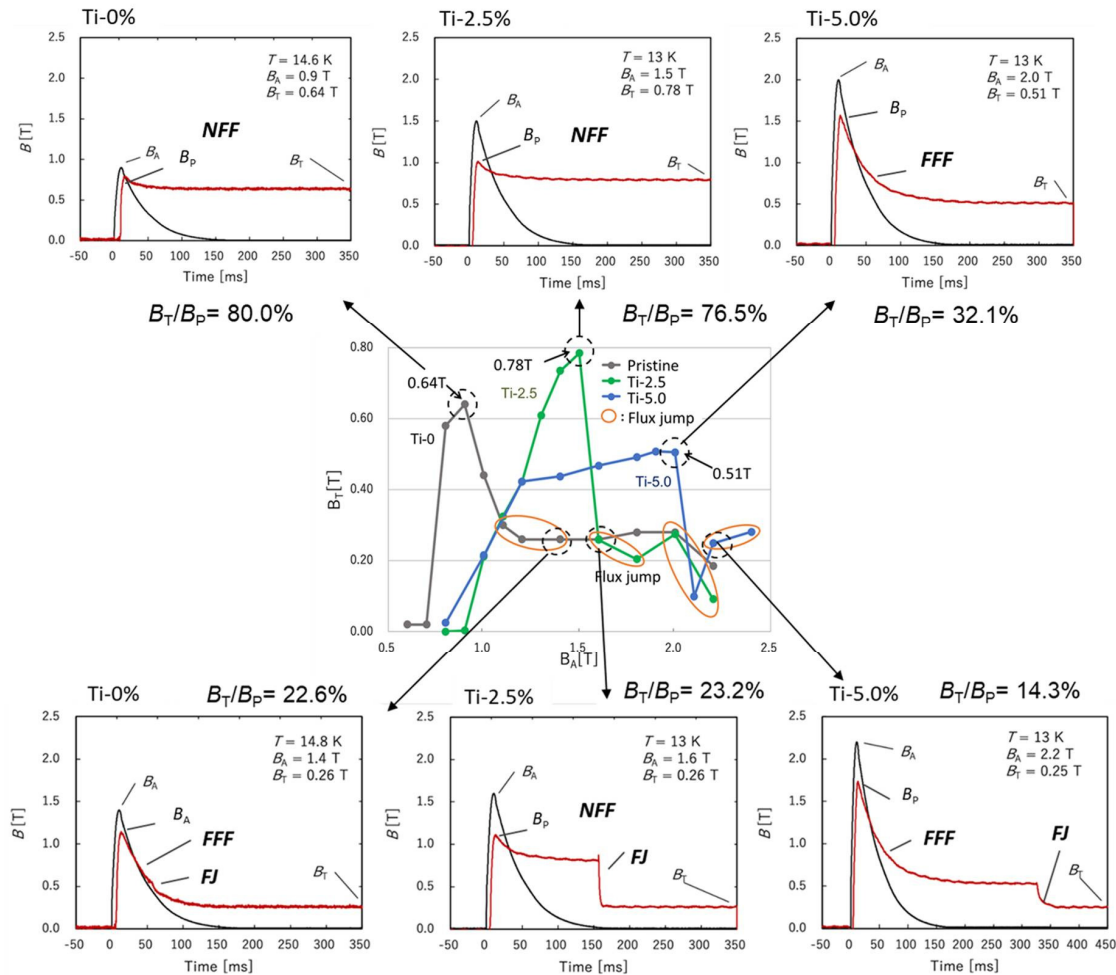


**Figure 6.** Evolutional profiles of field trapping.

Ti-added samples. This implies that Ti addition enhanced the shielding effect, as well as shown in Figure 3. The highest trappings were observed at 0.78 T at 1.5 T application for Ti 2.5% sample.

When we inspect Figure 5, the field trapping ratios  $B_T/B_P$  kept their values around 80% in the range from 1.0-1.5 T, exhibiting NFF. This suggests that the NFF region shifted to the high field region with increasing Ti addition. Although Ti-2.5wt% addition was apparently effective to shift the flux-invasion to the high field area, the  $B_T$  elevation was limited up to 0.78 T. Ti-5.0wt% addition has shown no advantages to improve  $B_T$ . However, Ti addition might have improved the thermal propagation, because we see no flux jumps even in the high field region less than 2.1 T. We must note that the Ti-addition shifts the NFF and FJ regions to high field region. If the thermal properties of the materials must have shifted by adding Ti, we should start the microstructural analysis in near future.

### 3.3 Flux jump in bulk $MgB_2$

The time dependent profiles in Figure 6 exhibit the clear classification to NFF, FFF, and FJ regions. NFF region gives us the most ideal flux trapping with less heat generation. FFF region suggests that the fast flux motion accompanied with heat generation slowly degrades the trapped fields. After FFF region, flux jumps suddenly happen with high speed and cause crucial heating in FJ regions.

When we carefully inspect the data, it is found that the PFM operation at the upper end of NFF region would decide the flux trapping performance. Since the FFF leads to FJ, it is important to keep and expand NFF region to high field areas. The experimental results clarified the secrets of Ti-doping as;

- ♦ No effects to enhance shielding against flux invasion
- ♦ Shifting the flux invasion to high field region
- ♦ Shifting the FJ area to high field region

When we inspect the FFF region we should anticipate the sudden FJ phenomena to happen.

In the future, we should try to develop the heat draining system and to improve the thermal properties like specific heat or heat propagation properties of material itself in order to suppress the temperature raise, and to expand the NFF region to the higher field.

### 3.4 Flux jump in bulk REBCO

The behavior of flux jumps is different between GdBCO and  $\text{MgB}_2$  magnets. In Figure 7, when single 7 T was applied, the trapped field  $B_T$  kept 3.2 T, showing a value of  $B_T/B_p = 64\%$ . In the case of multi-pulse application, the  $B_T$  of 1.2 T was trapped after the first field application of 5 T, showing a M-shape field distribution [19]. When a following 7 T was applied, the  $B_p$  jumped up to 6 T. This flux motion caused substantial heat at the surface center of the sample. This brought a sudden flux jump at an early time of 40 ms even at 30 K.

In general, REBCO bulk is as far stable against flux jumps to occur. Inhomogeneous microstructure of GdBCO would make the flux motion complex in comparison with homogeneous  $\text{MgB}_2$ . Since high specific heat and low heat propagation of GdBCO suppress the heat transfer from the heating point to the surface center where Hall sensor is attached, we can detect the flux jump which happens near the center. Then, we observe it at the time just after the peak of  $B_p$ . This means that the heat propagation must attributed to the detection of flux jump. In  $\text{MgB}_2$ , magnetic flux jumps happen quite late from the beginning of field application. Local heat generation and rapid heat propagation of bulk  $\text{MgB}_2$  are attributed to the flux jump behavior.

## 4. Conclusion

Through the PFM procedure conducted at 30 K, the authors have estimated the magnetic flux-trapping property of  $\text{MgB}_2$  samples bearing various Ti-contents made by hot pressing in IFW Dresden. Time dependence of the flux motion revealed the effect of Ti addition. The parameter of field trapping ratios  $B_T/B_p$  led us to the understanding of the flux motion during PFM, which showed us three classification as NFF, FFF, and FJ regions. Since the highest field trapping appears at the end point of NFF region, we should attempt to expand the NFF region as far as high field area before FFF region come out, which brings the FJ region. We compared the flux motion and flux jump in GdBCO bulk sample. We observed a flux jump due to substantial heat generation when the pulsed field of 7 T changed the trapped field distribution from the preactivated M-shaped to conical distribution, showing its superior stability than bulk  $\text{MgB}_2$ .

## Acknowledgments

This work has been partially supported by the project named as Strategic Young Researcher Overseas Visits Program for Accelerating Brain Circulation of JSPS.

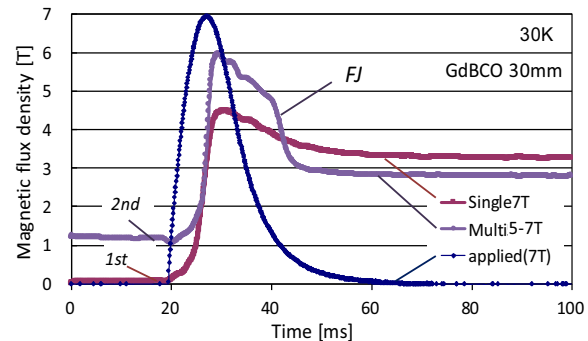


Figure 7. Flux trapping and flux jump in GdBCO.

## References

- [1] Weinstein R, Chen In-Gan, Liu J and Lau K 1991 Permanent magnets composed of high temperature superconductors *J. Appl. Phys.* **70** 6501
- [2] Murakami M 2007 Processing and Applications of Bulk RE–Ba–Cu–O Superconductors *Int. J. Appl. Ceram. Technol.* **4** 225
- [3] Durrell J, Dennis A, Jaroszynski J, Ainslie M, Palmer K, Shi Y-H, Campbell A, Hull J, Strasik M, Hellstrom E and Cardwell D 2014 A trapped field of 17.6 T in melt-processed bulk Gd-Ba-Cu-O reinforced with shrink-fit steel *Supercond. Sci. Technol.* **27** 082001
- [4] Fuchs G, Häbler W, Nenkov K, Scheiter J, Perner O, Handstein A, Kanai T, Schults L and Holzapfel B 2013 High trapped fields in bulk MgB<sub>2</sub> prepared by hot-pressing of ball-milled precursor powder *Supercond. Sci. Technol.* **26** 122002
- [5] Tateiwa T, Sazuka Y, Fujishiro H, Hayashi H, Nagafuchi T and Oka T 2007 Trapped field and temperature rise in rectangular-shaped HTSC bulk magnetized by pulse fields *Physica C* **463-465**, 398
- [6] Fujishiro H, Mochizuki H, Ainslie M D and Naito T 2016 Trapped field of 1.1 T without flux jumps in an MgB<sub>2</sub> bulk during pulsed field magnetization using a split coil with a soft iron yoke *Supercond. Sci. Technol.* **29** 084001
- [7] Mizutani U, Mase A, Ikuta H, Yanagi Y, Yoshikawa M, Itoh Y and Oka T 1999 Synthesis of c-axis oriented single-domain Sm123 superconductors capable of trapping 9 Tesla at 25 K and its application to a strong magnetic field generator *Mat. Sci. Eng.* **B65** 66
- [8] Ikuta H, Yanagi Y, Yoshikawa M, Ito Y, Oka T and Mizutani U 2001 Melt processing and the performances as a superconducting permanent magnet of RE-Ba-Cu-O/Ag (RE=Sm, Nd) *Physica C* **357-360** 837
- [9] Oka T 2007 Processing and Applications of Bulk HTSC *Physica C* **463-465** 7
- [10] Murakami A, Teshima H, Naito T, Fujishiro H and Kudo T 2014 Mechanical Properties of MgB<sub>2</sub> Bulks *Phys. Procedia* **58** 98
- [11] Nakamura T, Itoh Y, Yoshikawa M, Oka T and Uzawa J 2007 Development of a Superconducting Magnet for Nuclear Magnetic Resonance Using Bulk High-Temperature Superconducting Materials *Concepts in Mag. Res. Part B (Mag. Res. Eng)* **31** 65
- [12] Ogawa K, Nakamura T, Terada Y, Kose K and Haishi T 2011 Development of a magnetic resonance microscope using a high  $T_c$  bulk superconducting magnet *Appl. Phys. Lett.* **98** 234101
- [13] Nagamatsu J, Nakagawa N, Muranaka T, Zenitani Y and Akimitsu J 2001 Superconductivity at 39 K in magnesium diboride *Nature* **410** 63
- [14] Yokoyama K, Katsuki A, Miura A and Oka T 2018 Comparison of trapped field characteristic of bulk magnet system using various type refrigerators *J. Phy. Conf. Ser.* **1054** 012072
- [15] Ainslie M, Zhou D, Fujishiro H, Takahashi H, Shi Y-H and Durrell J 2016 Flux jump-assisted pulsed field magnetisation of high- $J_c$  bulk high-temperature superconductors *Supercond. Sci. Tech.* **29** 124004
- [16] Miyazaki T, Fukui S, Ogawa J, Sato T, Oka T, Scheiter J, Häbler W, Kulawansha E, Zhao Y and Yokoyama K 2017 Pulse field magnetization for disc-shaped MgB<sub>2</sub> Bulk Magnets *IEEE Trans. Appl. Supercond.* **27** 6800504
- [17] Oka T, Takeda A, Sasaki S, Ogawa J, Fukui S, Sato T, Scheiter J, Häbler W, Katsuki J, Miura A and Yokoyama K 2018 Magnetic Flux Invasion and Field-Capturing in Pulsed-Field Magnetization for Layered MgB<sub>2</sub> Bulk Magnets *IEEE Trans. Appl. Supercond.* **28** 6800504
- [18] Oka T, Takeda A, Oki H, Ogawa J, Fukui S, Sato T, Scheiter J, Häbler W, Katsuki J, Miura A and Yokoyama K 2019 Study on Magnetic Flux Dissipation and Field-Trapping Performance of HTS Bulk-Shaped Magnesium Diboride in Pulse-Field Magnetizing Processes *IEEE Trans. Appl. Supercond.* **29** 6802606
- [19] Oka T, Hara K, Takeda A, Ogawa J, Fukui S, Sato T, Yokoyama K and Murakami A 2017 Magnetic flux invasion in REBCO bulk magnets with varying pre-magnetized flux distributions in multiple-PFM processes *J. Phy. Conf. Ser.* **871** 012049